Impulsive Fracture of Silicon by Elastic Surface Pulses with Shocks

A. M. Lomonosov and P. Hess

University of Heidelberg, Institute of Physical Chemistry, Im Neuenheimer Feld 253, 69120 Heidelberg, Germany

(Received 30 May 2002; published 13 August 2002)

During nonlinear evolution of surface acoustic waves (SAWs) stress increases with propagation, and may cause fracture of brittle materials. This effect was used to evaluate the strength of crystalline silicon with respect to impulsive load in the nanosecond time scale without using seed cracks. Short SAW pulses propagating in the $[\bar{1}\bar{1}2]$ direction on the Si(111) plane induce fracture at significantly lower SAW amplitudes than the mirror symmetric wave propagating in the $[11\bar{2}]$ direction. This effect is explained by the differences in elastic nonlinearity of the two propagation directions.

DOI: 10.1103/PhysRevLett.89.095501 PACS numbers: 62.20.Mk, 43.25.+y, 62.30.+d, 68.35.Ja

The development of a realistic picture of the initiation and progress of bond-breaking processes in brittle solids is not only of basic scientific interest but also of immense practical importance. Even the most perfect crystals, such as silicon, may contain various structural defects, e.g., dislocations, microcracks, or microscopic impurities, which control the mechanical strength. Microscopic approaches, such as lattice theory, which characterize bond breaking at the atomic level, are available; however, the information obtained on the behavior of real materials is very limited [1]. Despite the fact that molecular dynamics simulations can now handle $\sim 10^7$ atoms on short time scales (tens of nanoseconds) this is by far not sufficient for a realistic description of the extended elastic field around the propagating tip of a crack and the analysis of long-term brittle fracture dynamics [2,3]. Since the theoretical treatment of the complex fracture process is extremely difficult, experimental results will play a dominant role in the future development of fracture mechanics.

Recent investigations of the mechanical strength of brittle silicon crystals have been performed using dynamic fracture experiments, in which the material is loaded with a constant force [4–7]. This tensile loading geometry generates a running crack starting at a preformed seed crack. With the ''potential drop'' method it is possible to measure the speed of cracks with an accuracy of up to 50 m/s, by measuring the change in resistance of the doped silicon wafer during crack propagation [5–7]. While continuum elasticity theory predicts that cracks should propagate at the Rayleigh velocity of the surface acoustic wave (SAW), the actual velocity observed for different loadings is only about 50%–85% of that value. Such substantial deviations are not surprising, since dynamic fracture is neither an elastic nor a continuous process.

In the present work we do not consider constant displacement boundary conditions resulting in steady-state fracture but transient or impulsive loading, as is usually encountered in practice. The nature of impulsive fracture dynamics is even more complex than the former case. Impulsive fracture can be realized by using nonlinear SAW pulses that develop shock fronts with increasing peak stress during propagation in a nonlinear medium. This is the distinguishing feature of surface waves, which is associated with the nonlocal character of the elastic nonlinearity in this case [8]. In sound waves with shocks propagating in a fluid, the pressure amplitude decreases with propagation. In this work we study the effect of SAW-induced fracture in crystalline silicon that occurs spontaneously along the weakest cleavage plane when the corresponding critical strain is reached in the tensile part of the surface pulse.

Excitation of straight-crested nonlinear SAWs was achieved by focusing the radiation of a pulsed Nd:YAG laser (1.06 μm, 8 ns, pulse energy <150 mJ) to a line at the surface using a cylindrical lens. The surface pulses were detected at two different distances from the source by probe beam deflection (PBD) monitored with a position sensitive detector. The probe laser was a diode-pumped cw Nd:YAG laser (532 nm, 100 mW). The setup had a bandwidth of about 500 MHz. To reach SAW amplitudes sufficient for the generation of strong shock fronts, a thin film of a highly absorbing carbon suspension was used at the source region [9,10]. With the PBD method the shear strain component of the SAW pulse $u_{31} = \partial u_3/\partial x_1$ at the free surface $x_3 = 0$ was measured at 3 and 18 mm distance from the source (Fig. 1), where u_3 is the normal surface displacement and the wave propagates along the x_1 axis.

The Si(111) plane and the $\langle 112 \rangle$ direction were selected for the experiments because of the high value of the coefficient of nonlinearity and the suppression of diffraction in this geometry. Moreover, the evolution of the SAW pulse can be accurately calculated, since the second- and third-order elastic constants are well known for silicon. Figure 2 shows the development of the $u_{3,1}$ profiles measured for SAW propagation in the $[11\bar{2}]$ and the $[\bar{1}\bar{1}2]$ directions on Si(111) at the two probe spots. The surprising effect of very different pulse shapes generated in the two opposing directions is explained by the symmetry properties of the selected plane and directions in the anisotropic silicon crystal, without referring to the fracture process itself, as previously suggested [10]. The nonlinear evolu-

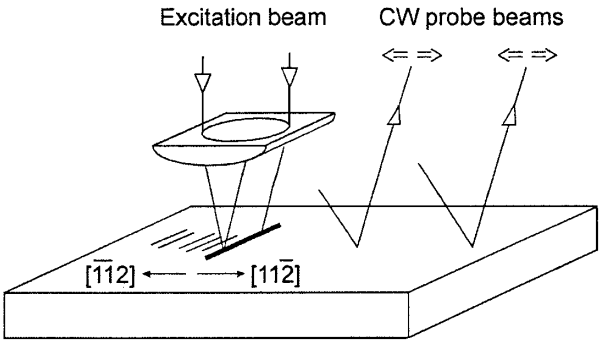

FIG. 1. Experimental setup used for detecting the effects of SAWs propagating in opposing directions [$11\bar{2}$] and [$\bar{1}\bar{1}2$] on the Si(111) plane after pulsed laser excitation.

tion of the SAW pulses is described by [11,12]:

$$i\frac{\partial}{\partial\tau}B_n = nq_0\Big[\sum_{0<n'<n} F(n'/n)B_{n'}B_{n-n'} + 2\sum_{n'>n}(n/n')F^*(n/n')B_{n'}B^*_{n'-n}\Big] - ibn^2B_n, \tag{1}$$

where B_n is the nth spectral amplitude, τ is the ''stretched'' coordinate along the direction of wave propagation, b describes the wave attenuation, and $q_0 = 2\pi/\Lambda$ is the fundamental wave number. The kernel F depends on the second- and third-order elastic constants, and thus describes the elastic nonlinearity of the medium. In anisotropic materials the nonlinear evolution and the stress field generated depend on the crystal plane and propagation direction. The silicon crystal is not symmetric about the (111) plane. This is manifested by a complex-valued kernel F, whereas for isotropic media and planes of symmetry in anisotropic crystals it is purely imaginary. Let us consider the two waves, 1 and 2, traveling in opposite directions, and therefore their spectral amplitudes are related by the complex conjugate $B_2 = B_1^*$. By substitution into Eq. (1), we find that the real part of F has opposite signs for these waves $F_1 = -F_2^*$. This results in opposite signs of the shock fronts and different stress distributions. As a consequence of these strongly deviating pulse shapes, the cracking behavior is expected to be different for the two directions.

To calculate the SAW profile at the second probe spot, the waveform measured at the first probe location is multiplied by a calibration factor, expanded into a Fourier series, and substituted into Eq. (1). By varying the calibration factor the duration of the simulated profile is fitted to the experimental N-type pulse of Fig. 2(a). The good agreement achieved between experiment and theoretical prediction confirms the usefulness of this calibration procedure. The profile of Fig. 2(b), possessing only one shock front, is not suitable for this purpose.

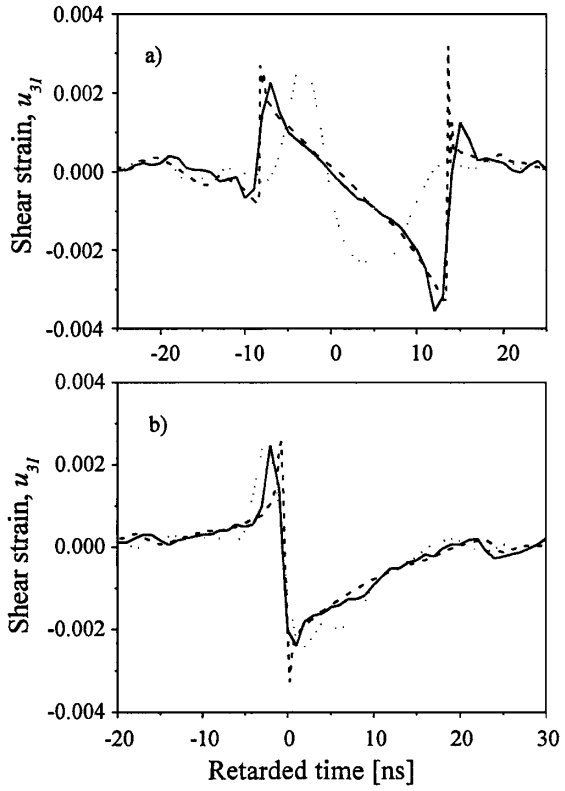

FIG. 2. Evolution of the nonlinear SAW profiles on Si(111) for pulses propagating in (a) the [$11\bar{2}$] direction and (b) the [$\bar{1}\bar{1}2$] direction. Dotted lines: waveforms measured at 3 mm; solid lines: waveforms measured at 18 mm; and dashed lines: calculated waveforms.

As one can see from Fig. 2, nonlinear evolution leads to the formation of short spikes in the vicinity of the shocks. Their duration was comparable to the sampling rate of the detection technique applied, or, in other words, the finite bandwidth of the setup limited the evaluation of the spike magnitude, and therefore the peak values of stress could be significantly larger than estimated from the measured waveforms. The growth of spikes is governed by the nonlinear term on the right-hand side of Eq. (1), and is limited by the attenuation term in this equation. As a shock front, which is accompanied by two spikes, becomes steeper, the dissipation, which is assumed to be proportional to the frequency squared, starts to play a dominant role. The strain spikes reach a maximum and then decrease with further propagation. Because of our experimental conditions we were not able to detect spikes shorter than 1 ns. In order to estimate the maximal strain we introduced the experimental value for the dissipation parameter b into Eq. (1) and integrated with the experimental initial condition over the propagation distance. The waveform obtained was determined solely by the nonlinearity and dissipation, and was independent of the properties of the SAW detection technique. Note that the calibration factor has to be determined independently. The attenuation of

ultrasonic waves in silicon was measured in [13] to be $\sim$1 dB/cm at the frequency $\omega = q_0 \nu_R = 350$ MHz. The simulations with this attenuation parameter are presented in Fig. 2. The predicted spikes are somewhat larger than the measured spikes, yielding a higher stress in the real SAW pulse.

Contrary to nonlinear elastic distortions in fluids, those in surface waves lead to an increase of stress with propagation, for example, in the form of spikes. This accumulation of stress is limited by the frequency-dependent damping process. If the characteristic shock formation length is small in comparison to the attenuation length $[2F(1/2)B_m q_m]^{-1} \ll (bm^2)^{-1}$, where m indicates the maximal spectral component, the stress accumulated after some distance reaches the mechanical strength of the materials, causing failure of the solid. With the absorbing layer technique employed here, acoustic Mach numbers (ratio of surface velocity to SAW phase velocity) between 10^{-3} and 10^{-2} are accessible. A further increase of the SAW amplitude is not possible due to spontaneous fracture.

The measured $u_{3,1}$ profiles, shown in Fig. 2, uniquely determine the complete wave field at any time and location in the sample. To evaluate this field we used the exact solution of the conventional linear elastic boundary problem. This provides a complete set of eigenvalues: the phase velocity, the depth distribution, and the polarization vectors for all partial waves involved. The $u_{3,1}$ profile is extended into a Fourier series, and the wave field $u_{ij}(x_1, x_3)$ is calculated as a sum of the wave fields of all spectral components. Then the stress tensor field $\sigma_{ij} = C_{ijkl} u_{k,l}$ is calculated, where C_{ijkl} designates the second-order elastic stiffness tensor. The stress tensor is then transformed to a new coordinate system connected with the actually observed $\{11\bar{1}\}$ cleavage plane of silicon. In this coordinate system the stress component σ_{11} represents an "opening" stress, directed normal to the cleavage plane. Because of the linear approximation applied, only small values of $u_{i,j}$ should be considered. This condition holds well in nonlinear SAWs, since the strains are limited by failure to the order of $\sim 10^{-2}$.

In Figs. 3(a) and 3(b) we display the calculated spatial-temporal distribution of the σ_{11} component for the two pulses presented in Figs. 2(a) and 2(b), respectively. A positive stress denotes stretching of the material, whereas a negative stress is associated with compression. Interestingly, the N-type pulse propagating in the $[11\bar{2}]$ direction exhibits two short compression peaks, while the $[\bar{1}\bar{1}2]$ pulse has one strong tensile peak. Thus the pulse formed in the $[\bar{1}\bar{1}2]$ direction is expected to induce fracture more easily along the weakest silicon cleavage plane than the one running in the opposite direction. Indeed, the SAW experiments reveal a significant difference in the conditions needed for crack induction. In the $[11\bar{2}]$ propagation direction, cracks were observed only for excitation laser pulse energies exceeding 120 mJ, whereas in the opposite direction the threshold was as low as 30 mJ. Under suitable conditions cracks appeared only on one side of the source, namely, in the $[\bar{1}\bar{1}2]$ direction, and the wave propagating in the $[11\bar{2}]$ direction could be used to measure the SAW amplitude. This was realized by gradually increasing the laser pulse energy until fracture was observed at the left side of the source, as indicated schematically in Fig. 1. Thus the SAW amplitude at the cracking threshold could be evaluated, yielding the critical tensile stress for the weakest cleavage plane. From the spatial-temporal distribution of the stress at the cracking threshold [Fig. 3(b)], a critical tensile stress of about 0.8 GPa was extracted for our silicon sample.

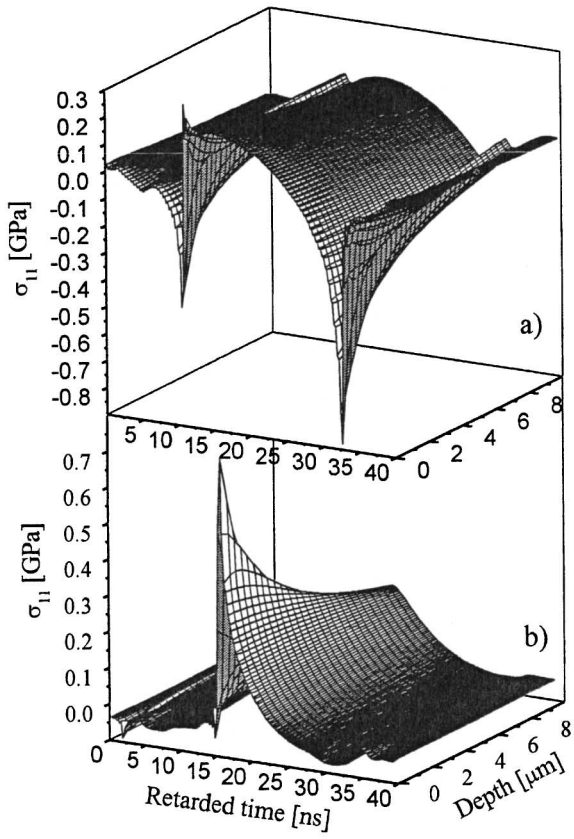

FIG. 3. Calculated spatial-temporal distribution of the σ_{11} component perpendicular to the cleavage plane for the pulse propagating in (a) the $[\bar{1}\bar{1}2]$ direction and (b) the $[11\bar{2}]$ direction.

SAW-induced cracks have been detected at the sample surface by scanning force microscopy, as shown in Fig. 4. A strongly nonlinear SAW pulse creates a whole series of cracks extending along the [110] direction perpendicular to the direction of SAW propagation. The characteristic sawtoothlike surface displacements observed are in the range of 10–30 nm with a separation of the individual cracks of 15–30 μm.

In summary, we succeeded in observing impulsive fracture of intrinsic silicon crystals without notching using the

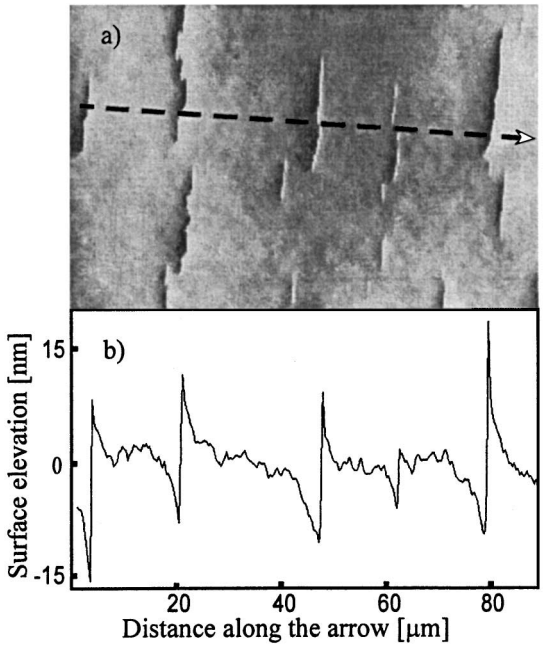

FIG. 4. (a) Scanning force microscopy image of the fractured Si(111) surface. The line indicates the position of the surface profile shown in (b) and the arrow is the direction of SAW propagation. (b) The cross section of the sample surface along the arrow.

effect of gradual growth of stress in the strongly nonlinear SAW pulses. On the Si(111) plane finite-amplitude SAWs propagating in the two opposing directions $[11\bar{2}]$ and $[\bar{1}\bar{1}2]$ develop very different nonlinear pulse shapes with strong compressive and tensile peaks, respectively, normal to the spontaneous $\{11\bar{1}\}$ cracking plane. The critical tensile stress of dynamic fracture of the weakest fracture plane was obtained from the calibrated shocks.

Financial support of this work by the Deutsche Forschungsgemeinschaft (DFG) is gratefully acknowledged.

[1] D. Holland and M. Marder, Adv. Mater. **11**, 793 (1999).
[2] S. J. Zhou, P. S. Lomdahl, R. Thomson, and B. L. Holian, Phys. Rev. Lett. **76**, 2318 (1996).
[3] F. F. Abraham, Phys. Rev. Lett. **77**, 869 (1996).
[4] D. Holland and M. Marder, Phys. Rev. Lett. **80**, 746 (1998).
[5] J. A. Hauch, D. Holland, M. Marder, and H. L. Swinney, Phys. Rev. Lett. **82**, 3823 (1999).
[6] T. Cramer, A. Wanner, and P. Gumbsch, Z. Metallkd. **90**, 675 (1999).
[7] T. Cramer, A. Wanner, and P. Gumbsch, Phys. Rev. Lett. **85**, 788 (2000).
[8] M. F. Hamilton, Yu. A. Ilínsky, and E. A. Zabolotskaya, J. Acoust. Soc. Am. **97**, 882 (1995).
[9] Al. A. Kolomenskii, A. M. Lomonosov, R. Kuschnereit, P. Hess, and V. E. Gusev, Phys. Rev. Lett. **79**, 1325 (1997).
[10] A. M. Lomonosov and P. Hess, Phys. Rev. Lett. **83**, 3876 (1999).
[11] A. P. Mayer, Phys. Rep. **256**, 237 (1995).
[12] A. M. Lomonosov, P. Hess, and A. P. Mayer, in *Modern Acoustical Techniques for the Measurement of Mechanical Properties*, edited by M. Levy, H. E. Bass, and R. Stern (Academic Press, San Diego, 2001), pp. 65–134.
[13] Yu. V. Ilisarskii and V. M. Sternin, Sov. Phys. Solid State **27**, 236 (1985).